

Influence of a Magnetic Field on Tunneling from a Type-II Alloy Superconductor*

W. J. TOMASCH

Atomics International Division of North American Aviation, Incorporated, Canoga Park, California

(Received 23 February 1965)

Planar tunnel diodes have been utilized to study the influence of longitudinal and transverse magnetic fields ($H_{||}$ and H_{\perp} , respectively) on electronic tunneling phenomena involving type-II superconducting alloys (1.1–4.2°K). Each diode consisted of a very thick Pb-Tl alloy film (2.5–7.5 μ , 4.3–13.5 at. % Tl) separated from a much thinner Al film (as thin as ≈ 200 Å) by an extremely thin (≈ 30 Å) natural aluminum oxide layer. Zero-field current-voltage (I - V) diode characteristics observed with the Al superconducting have demonstrated the existence of a sharply defined alloy energy gap which is essentially independent of alloy composition. With the Al superconducting, very high diode impedances were observed in longitudinal fields for voltages exceeding half the zero-field Al energy gap, suggesting that very nearly all of the alloy surface retains a nonzero energy gap to at least twice the bulk thermodynamic critical field H_c . Furthermore, a form of sharp I - V structure persisted to values of $H_{||}$ satisfying $H_{c1} < H_{||} < 2H_c$, where H_{c1} is the Abrikosov lower critical field. This structure has been interpreted tentatively in terms of a field-induced distribution of alloy energy gaps $2\epsilon_i$ satisfying $\epsilon_m \leq \epsilon_i \leq \epsilon_M$, where ϵ_m is the distribution minimum, probably corresponding to the value at the surface, and ϵ_M is the distribution maximum, which approximately equals the zero-field half energy gap. In transverse fields, evidence of superconductivity in the alloy ceases at $H_{\perp} = H_t$, which correlates well numerically with bulk values of the Abrikosov upper critical field H_{c2} . In longitudinal fields, however, evidence of superconductivity was observed to persist to H_t , where H_t/H_c ranges between 1.7 and 1.9 depending on alloy composition. The present results indicate rather directly that in longitudinal fields superconductivity persists beyond H_{c2} within a few coherence lengths of the surface, and extends over a major fraction of the surface. Furthermore, the numerical value of H_t/H_c is in reasonable accord with the *sheath* critical field ratio predicted by Saint-James and de Gennes for longitudinal fields. For transverse fields, they predict that the sheath will not appear above H_{c2} , consistent with present observations. Taken as a whole, the present measurements are believed to be typical of *bulk* specimens for which flux entry is delayed to fields substantially greater than H_{c1} because of surface smoothness.

I. INTRODUCTION

QUASIPARTICLE tunneling phenomena (Giaever tunneling)^{1,2} have been utilized with great efficacy in the study of type-I elemental superconductors ($H_{c2} < H_c$) for the case of zero applied magnetic field. In brief, the following features of the quasiparticle density of states $N(E)$ have been ascertained by means of tunneling experiments: (1) a precise knowledge of the energy gap as a function of temperature,^{1–12} (2) the specific functional form of $N(E)$,^{1,3,7,12,13} and (3) the influence of the lattice phonon spectrum upon $N(E)$.^{7,12,14–17} For longitudinal magnetic fields, similar

experimental methods have been employed to study very thin films of elements which are type I in the bulk, but which exhibit a second-order phase transformation in the presence of a field by virtue of film thinness.^{3,18,19} Interpretation of such measurements is greatly facilitated by the fact that very thin films exhibit a unique (single) energy gap, just as do thicker films in zero field. A few measurements have also been performed on films of type-I material sufficiently thick so as to avoid size effects.^{20,21}

In the absence of a field, there appears to be little difficulty in extending these same techniques to the case of type-II alloy superconductors ($H_{c2} > H_c$) since the observed I - V diode characteristics²⁰ are quite similar to those obtained previously^{1,2} (type I) and are easily interpreted in terms of a unique energy gap model. In the presence of a field, however, this situation is altered substantially,^{20,22,23} posing a nontrivial interpretive problem. Several simple methods for extracting information from the observed I - V characteristics will be introduced.

* Work supported by the U. S. Atomic Energy Commission.

¹ I. Giaever, Phys. Rev. Letters **5**, 147, 464 (1960).

² J. Nicol, S. Shapiro, and P. H. Smith, Phys. Rev. Letters **5**, 461 (1960).

³ Ivar Giaever and Karl Megerle, Phys. Rev. **122**, 1101 (1961).

⁴ M. D. Sherrill and H. H. Edwards, Phys. Rev. Letters **6**, 460 (1961).

⁵ N. V. Zavaritskii, Zh. Eksperim. i Teor. Fiz. **41**, 831 (1961)

[English transl.: Soviet Phys.—JETP **14**, 470 (1961)].

⁶ N. V. Zavaritskii, Zh. Eksperim. i Teor. Fiz. **43**, 1123 (1962)

[English transl.: Soviet Phys.—JETP **16**, 793 (1963)].

⁷ I. Giaever, H. R. Hart, Jr., and K. Megerle, Phys. Rev. **126**, 941 (1962).

⁸ S. Shapiro, P. H. Smith, J. Nicol, J. L. Miles, and P. F. Strong, IBM J. Res. Develop. **6**, 34 (1962).

⁹ D. H. Douglass, Jr., IBM J. Res. Develop. **6**, 44 (1962).

¹⁰ P. Townsend and J. Sutton, Phys. Rev. **128**, 591 (1962).

¹¹ D. H. Douglass, Jr. and R. Meservey, Phys. Rev. **135**, A19 (1964).

¹² S. Bermon and D. M. Ginsberg, Phys. Rev. **135**, A306 (1964).

¹³ P. Townsend and J. Sutton, Phys. Rev. Letters **11**, 154 (1963).

¹⁴ J. M. Rowell, A. G. Chynoweth, and J. C. Phillips, Phys. Rev. Letters **9**, 59 (1962).

¹⁵ J. M. Rowell, P. W. Anderson, and D. E. Thomas, Phys. Rev. Letters **10**, 334 (1963).

¹⁶ J. M. Rowell and L. Kopf, Phys. Rev. **137**, A907 (1965).

¹⁷ J. G. Adler and J. S. Rogers, Phys. Rev. Letters **10**, 217 (1963).

¹⁸ D. H. Douglass, Jr., Phys. Rev. Letters **7**, 14 (1961).

¹⁹ R. Meservey and D. H. Douglass, Jr., Phys. Rev. **135**, A24 (1964).

²⁰ W. J. Tomasch, Bull. Am. Phys. Soc. **8**, 419 (1963).

²¹ Y. Goldstein, Phys. Letters **12**, 169 (1964); Proceedings of the Ninth International Conference on Low Temperature Physics, 1964 (to be published).

²² W. J. Tomasch, Phys. Letters **9**, 104 (1964).

²³ W. J. Tomasch, Proceedings of the Ninth International Conference on Low Temperature Physics, 1964 (to be published).

In qualitative terms, however, it is possible to anticipate the more prominent features of information potentially accessible to tunneling. Although a thick film may be thought of as being bulk matter insofar as geometrical size effects are concerned, the high probability that tunneling electrons originate within a surface layer approximately a mean free path in depth implies that the information available characterizes a relatively small volume of the specimen which may not be typical of the specimen as a whole. Hence, it is not unreasonable to suppose that tunneling phenomena may serve as a sensitive probe for the study of surface (sheath) effects associated with bulk specimens, whereas these are easily missed in many other types of experiments performed with bulk specimens owing to the small volume fraction involved. On the other hand, the energy gap should tend to achieve its limiting interior behavior near the inner boundary of this same surface layer owing to the fact that the coherence length and the mean free path are approximately equal for the present experimental conditions. It is not surprising, therefore, that experimental results for modest longitudinal fields ($H_{11} \approx H_{c1}$) are interpretable in terms of a distribution of energy gaps having an upper bound approximately equal to the zero-field alloy energy gap. Since the electrons of interest originate from within a transitional layer, insulator at one boundary and bulk superconductor at the other, it would appear that tunneling experiments could in principle yield insight into both surface and interior aspects of superconductivity.

II. SURVEY OF EXPERIMENTAL PHENOMENA AND METHODS OF DATA PRESENTATION

A. Aluminum Superconducting

As indicated in Figs. 1 and 2, $I-V$ plots obtained in zero field are characteristic of electronic tunneling be-

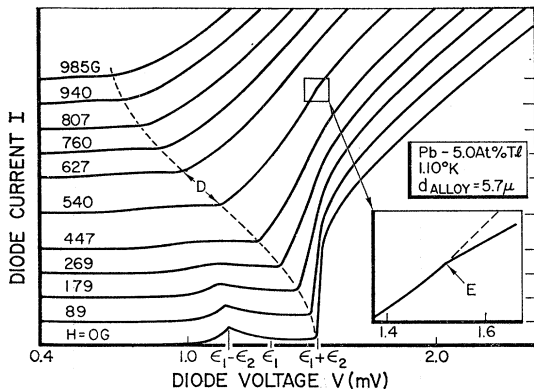


FIG. 1. Effects of longitudinal magnetic fields on diode junction $I-V$ characteristics when both alloy and Al are superconducting. Indicated values of ϵ_1 and ϵ_2 correspond, respectively, to half-energy gaps of alloy and Al in zero field. Inset discloses persistence of structure at $V_B \approx \epsilon_1(0) + \epsilon_2(0)$. Note constant suppression of voltage zero. The current zero of every curve ($H > 0$) has been displaced, and intersections with the I axis correspond to $I=0$ within experimental accuracy.

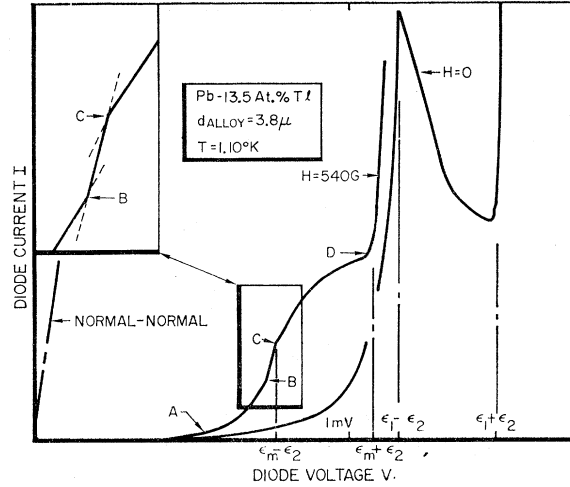


FIG. 2. Modification of the negative differential conductance region produced by a longitudinal magnetic field. Line labeled normal-normal indicates ohmic diode response when superconductivity has been quenched magnetically in both alloy and Al. Inset presents an expanded view of structure. Quantities $\epsilon_m(H)$ and $\epsilon_2(H)$ are interpreted as the alloy minimum half energy gap and the Al half energy gap, respectively.

tween two superconductors, each of which exhibits a sharply defined energy gap. Consequently, the alloy energy gap $2\epsilon_1(H=0)$ may be determined in the usual way^{1,2} and may be studied as a function of alloying.

Upon application of a longitudinal field, the constant-field $I-V$ curves are soon altered to an extent which precludes use of the usual methods for identifying $\epsilon_1(H)$. The initial region of negative differential conductance ($H=0$) evolves continuously into a smooth, plateau-like region which continually becomes less prominent as it shifts to lower values of V , as in Fig. 1. Despite this trend, certain structural features persist to significantly high fields, provided that sufficiently thin Al films are employed so that the Al itself remains superconducting. Under conditions of high gain and low noise ($\approx 20 \mu V$), fairly sharp changes in slope are consistently observed at the leading edge of the plateau (features B and C of Fig. 2) as well as near the zero-field value of $V = \epsilon_1 + \epsilon_2$ (feature E of Fig. 1), where ϵ_2 is the Al energy gap. Finally, the rapid rise in I which marks the end of the plateau region (feature D of Figs. 1 and 2) also occurs at a reasonably well-defined value of V . As will be seen, these features appear to be explicable in terms of a model based on a field-induced distribution of energy gaps within the surface layer of the alloy. For reasons which will become clear, the quantitatively important aspects of the situation may be characterized via the potentials $\epsilon_m = \frac{1}{2}(V_D + V_C)$, $\epsilon_2 = \frac{1}{2}(V_D - V_C)$, and $\epsilon_M = (V_B - \epsilon_2)$. For the particular diodes studied, the residual structure just described (V_B, V_C, V_D , and V_E of Figs. 1 and 2) was lost before attainment of roughly one-quarter of the field required to quench all superconductivity as evidenced by tunneling.

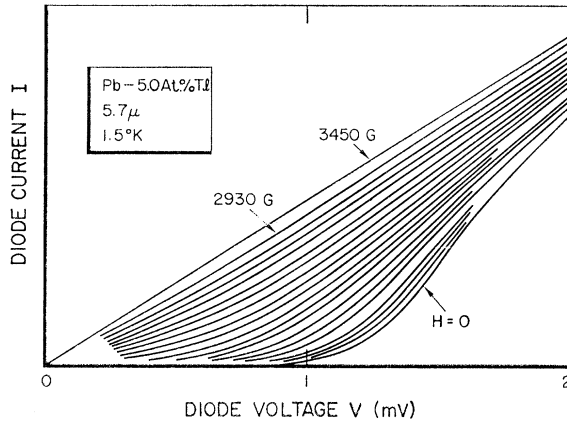


FIG. 3. Effect of longitudinal magnetic fields on diode junction I - V characteristics when only alloy is superconducting. Straight line (3450 G) corresponds to complete magnetic quenching of superconductivity in alloy (Ohmic limit).

B. Aluminum Normal

In zero field, the I - V plots obtained are typical of tunneling between a normal metal (Al) and a superconductor (alloy), the latter exhibiting a reasonably sharp energy gap (Fig. 3). A moderate amount of thermal smoothing is present due to the necessity of maintaining the temperature slightly above the critical temperature of the Al films ($T_C \approx 1.4^\circ\text{K}$). Application of a longitudinal field generates a continuous family of curves which approach the Ohmic limit for $H_{||} = H_{\perp} \approx (1.7-1.9) \times H_{c2}(\text{bulk})$. A similar family is generated by the application of a transverse field, the Ohmic limit being attained when the condition $H_{\perp} = H_{||} \approx H_{c2}(\text{bulk})$ is satisfied. Although superconductivity persists to these high fields (both for $H_{||}$ and H_{\perp}), it is quite likely that electronic states are introduced into the energy gap at substantially lower fields, i.e., the alloys become "gapless" superconductors.²⁴⁻²⁶ This is reflected in the fact that the differential conductance at $V=0$ becomes nonzero at fields substantially lower than H_{\perp} or $H_{||}$.

Although I - V characteristics with the Al superconducting can yield quantitative energy gap information quite directly so long as V_C and V_D remain defined, beyond this point they appear to have little advantage over those obtained with the Al normal. Three simple schemes will be considered for quantitatively characterizing the "degree" of superconductivity reflected in the data of Fig. 3. These are presented in Fig. 4. The first is just the area $A(H)$ between the Ohmic limit and any curve of constant H . As will be seen, simple arguments can be made which appear to indicate that $A(H)$ is

²⁴ A. A. Abrikosov and L. P. Gor'kov, Zh. Eksperim. i Teor. Fiz. 39, 1781 (1960) [English transl.: Soviet Phys.—JETP 12, 1243 (1961)].

²⁵ F. Reif and Michael Woolf, Phys. Rev. Letters 9, 315 (1962); Phys. Rev. 137, A557 (1965).

²⁶ P. Burger, G. Deutscher, E. Guyon, and A. Martinet, Proceedings of the Ninth International Conference on Low Temperature Physics 1964 (to be published).

nearly proportional to the square of an average energy gap, at least in the limit of small fields and low temperatures. Within the validity of such reasoning, $A(H)$ should be roughly proportional to the average condensation energy remaining in the surface layer,²⁰ since the density of states at the Fermi level $N(0)$ does not appear to be a strong function of alloying. A second method utilizes a profile parameter²² $P(V, H)$ which has been defined graphically in Fig. 4. Since P is by definition evaluated at a fixed value of V (constant displacement of the Fermi potential across the diode junction), a uniform method of specifying V for any given alloy would be highly desirable. Beyond its intuitive appeal, the selection of $V = \epsilon_1(H=0)$ is recommended by the fact that $\epsilon_1(H=0)$ (as obtained from tunneling data) is essentially composition-independent, and that this particular choice of V more or less maximizes the magnitude of certain structural features of P to be discussed shortly. (It should be noted that a somewhat different choice for V would not change the behavior of P in any essential way.) In the future, P will be understood to have been evaluated at $\epsilon_1(H=0)$. Finally, the initial differential conductance ($V=0$) may be utilized via the parameter $\Phi(H) = (\tan\phi_0 - \tan\phi)$ as in Fig. 4. For purposes of comparison, all three parameters have been normalized to unity at $H=0$. A semi-quantitative resumé of the field dependence of $A_{||}$, $P_{||}$, and $\Phi_{||}$, as well as of P_{\perp} , is presented in Fig. 5. Within limits of experimental uncertainty, the field value at which all three parameters vanish is the same as that

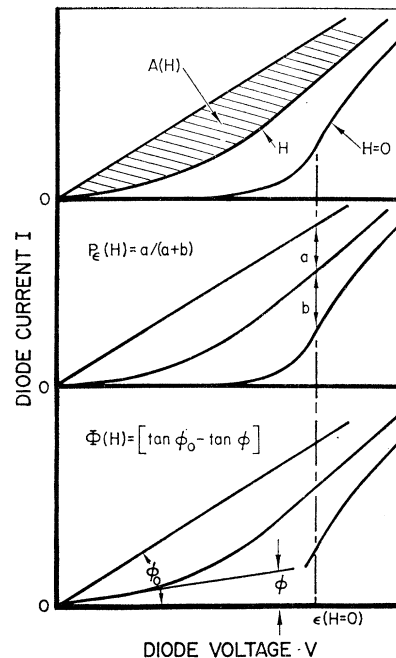


FIG. 4. Three methods for quantitatively characterizing the degree of superconductivity reflected in the data of Fig. 3. Quantities A and P are referred to as the area and profile parameters, respectively.

required for the onset of electrical resistance in the alloy film. The cessation of superconductivity as evidenced by tunneling appears to coincide with the final return of the alloy to the normal state. An immediate consequence is the definition of two critical fields H_l and H_t , as in Fig. 5. Both fields are observed to be well-behaved experimental quantities with magnitudes determined by temperature and alloy composition. In particular, H_t is found to agree well with bulk values of H_{c2} as determined from bulk magnetization data,²⁷⁻²⁹ while H_l falls in the interval $1.7H_{c2} < H_l < 1.9 H_{c2}(\text{bulk})$.

Figure 5 also indicates that A_{11} , P_{11} , and Φ_{11} display reasonably localized changes in slope at two fairly well-defined fields below H_l . The higher field value correlates reasonably well with H_t while the lower value falls in the range $H_{c1}(\text{bulk}) \leq H_x \leq H_c(\text{bulk})$. The fact that all three parameters are still quite sizeable at $H_{c2}(\text{bulk})$, when magnetization studies²⁷⁻²⁹ indicate that bulk matter is restored to the normal state, presumably points to the existence of surface superconductivity. In practice, the sharp features of Fig. 5 are somewhat more rounded. (It is interesting to note the general resemblance between P_{11} and A_{11} since the former characterizes the effect of a longitudinal field for a constant displacement of the Fermi potential across the diode junction, while the latter averages the effect over a range of displacements which is large compared to the alloy energy gap.) Figure 6 displays the manner in which A_{11} and P_{11} reflect the superconducting-to-normal (S-N) transition of a thick Pb film subject to a longitudinal field. The extremely abrupt drop in both $A_{11}^{1/2}$ and P_{11} at the bulk value of H_c is believed to be typical of a first-order transformation as evidenced by tunneling. Surface phenomena are believed to be responsible for the tail

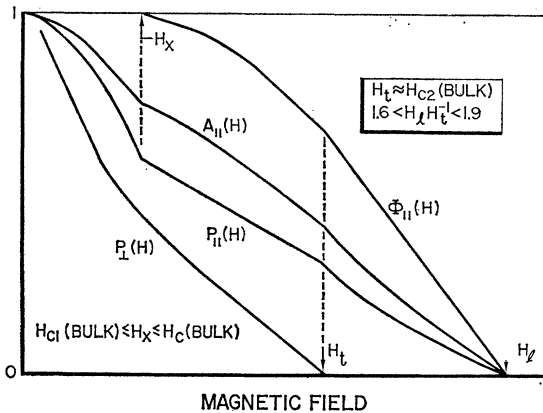


FIG. 5. A semiquantitative resumé of the field dependence of A_{11} , P_{11} , Φ_{11} , and P_{\perp} . Structural features have been emphasized somewhat for clarity. Parameters A_{11} , P_{11} , and Φ_{11} suffer a localized change in slope near H_x and H_t .

²⁷ G. Bon Mardion, B. B. Goodman, and A. Lacaze, Phys. Letters 7, 321 (1962).

²⁸ J. D. Livingston, Phys. Rev. 129, 1943 (1963).

²⁹ R. H. Kernohan and S. T. Sekula, Bull. Am. Phys. Soc. 9, 572 (1964).

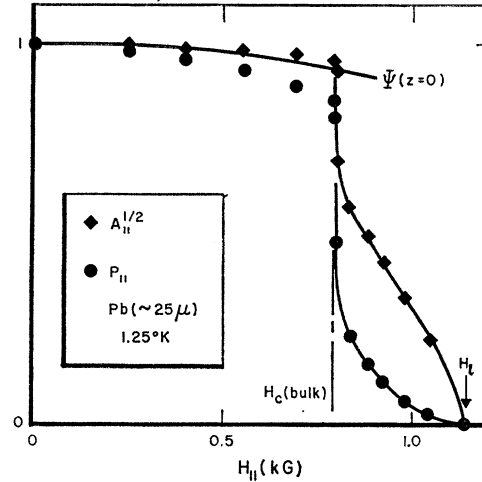


FIG. 6. Field dependence of $A_{11}^{1/2}$ and P_{11} for a thick Pb film. The curve for $H_{11} < H_c(\text{bulk})$ is the calculated G-L low-field order parameter $\Psi(z=0)$ (see footnotes 37 and 41). The fact that $A_{11}^{1/2}$ and P_{11} are nonzero for $H_c < H_{11} < H_t$ is attributed to surface superconductivity.

above $H_c(\text{bulk})$. Pure Pb appears capable of exhibiting a stable sheath phase ($H_{c3} > H_c$) but not a stable mixed phase ($H_{c2} < H_c$).^{21,30,31} Owing to the small number of diodes on which $\Phi_{11}(H)$ data were obtained, only A_{11} , P_{11} , and P_{\perp} data will be utilized in future discussion.

Finally, it should be noted that the present investigation has bent to use only the simplest experimental techniques for studying the effects of an applied magnetic field. It is quite likely that techniques previously employed by others to study type-I superconductors in zero field may also be applied to the present class of problems with advantage. In particular, direct and continuous displays of the differential conductance^{7,15} and its voltage derivative,¹⁵ as well as certain sensitive quantities such as P_{11} , versus applied diode voltage are likely to be of considerable value.

III. SPECIMEN PREPARATION AND MEASUREMENT METHODS

Six cruciform diode structures³ were fabricated at one time by means of standard evaporation techniques. Films were deposited upon room-temperature glass substrates, ambient pressures being typically $2-7 \times 10^{-7}$ mm Hg with deposition rates of $50-100 \text{ \AA sec}^{-1}$. Triple-stranded tungsten wire baskets served as the Al vapor source, while tungsten boats were utilized for the alloy source, both being Ohmically heated. Alloy source charges consisted of approximately 30 g of Pb doped with no more than 2 at.% Tl. All evaporants had an initial purity of 99.999 wt.% according to the supplier (American Smelting and Refining Company). Compositional homogeneity of the alloy films was monitored by

³⁰ B. Rosenblum and M. Cardona, Phys. Letters 9, 220 (1964).

³¹ Myron Strongin, Arthur Paskin, Donald G. Schweitzer, O. F. Kammerer, and P. P. Craig, Phys. Letters 12, 422 (1964).

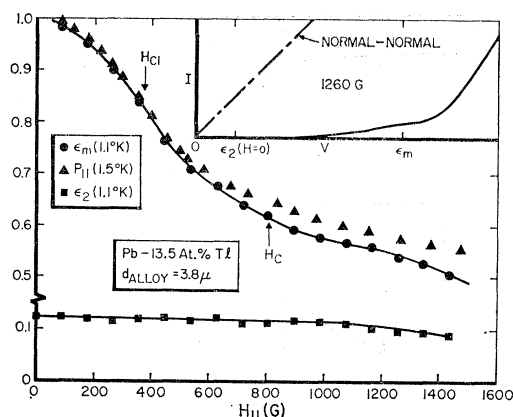


FIG. 7. Field dependence of $\epsilon_m(H_{||})$, $\epsilon_2(H_{||})$, and $P_{||}$. Inset displays I - V characteristic at 1260 G, emphasizing the very high-diode resistance above $\epsilon_2(H=0)$, the Al half-energy gap in zero field. Line labeled normal-normal indicates Ohmic response when all superconductivity has been quenched magnetically. Note contraction of ordinate between 0.1 and 0.5.

exposing additional glass substrates for only a fraction of the total evaporation period. Polarographic analysis of such substrates together with substrates exposed during the total period yielded a knowledge of the compositional gradient as well as the average specimen composition. By evaporating only a small fraction of the source charge, the change in alloy film composition over a distance of the order of a mean free path could be reduced to a negligibly small amount, as indicated in Table I. Thicknesses were calculated from wet-chemical mass determinations performed on specimens of known area, and assuming the bulk mass density of pure Pb, a very good approximation for this alloy system at the present thicknesses and concentrations. Aluminum oxide barrier layers were formed by exposing freshly evaporated Al films to air for several minutes.³ Due to the rapid deterioration of Pb-Tl films when exposed to air, it was necessary to store diodes in evacuated glass ampoulets or in a rough vacuum ambient (1–5 μ Hg). (Encapsulated diodes stored for a little over a year were found to yield quite satisfactory I - V plots.)

Diodes were studied in the four terminal configuration,³ power being supplied by a simple battery voltage source. After amplification (≈ 1000), the I - V signals were displayed on an X - Y recorder. An oscilloscope of

TABLE I. Description of alloy films.

Concentration at tunneling surface (at. % Tl)	Thickness (μ)	Concentration gradient (at. % Tl per 0.1 μ)
3.1
4.3	7.5	0.012
5.0	5.7	...
7.9	4.4	0.066
9.4	8.5	0.028
9.6	2.5	0.045
13.5	3.8	0.075

10 μ V/cm sensitivity, connected directly across the diode voltage probes, continuously monitored the ac pickup voltage. In order to observe sharp structure in the I - V characteristics, it is necessary to maintain low pickup levels at all times. Magnetic fields were supplied by a small Nb₃Zr superconducting solenoid. Both diode and solenoid were immersed in the same liquid helium bath, temperatures being determined from the helium vapor pressure. The solenoid was not operated in the persistent mode. It is estimated that alignment errors between the diode plane and applied longitudinal fields did not exceed two-tenths of a degree. A planimeter was used to make I - V area determinations.

IV. EXPERIMENTAL RESULTS

A. Aluminum Superconducting

Diode I - V characteristics typical of those obtained for the three compositions studied in detail (5.0, 7.9, and 13.5 at. % Tl) are presented in Figs. 1 and 2. The ϵ_m and ϵ_2 data of Fig. 7 are also representative. Very good reproducibility was observed from run to run, as well as between measurements made on several diodes which had been fabricated simultaneously. The bulk critical field values $H_{c1}(1.5^\circ\text{K})$ and $H_c(1.5^\circ\text{K})$ indicated in Fig. 7 were obtained from 4.2° bulk magnetization data^{27–29} on the assumption of a parabolic dependence on reduced temperature.³² As indicated by the

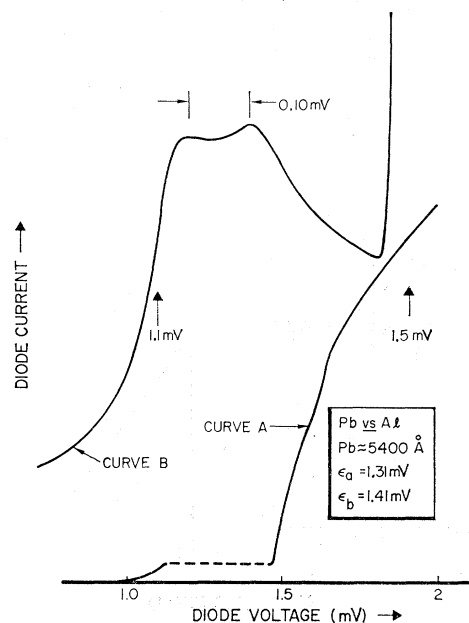


FIG. 8. Double energy gap of pure Pb as reflected in the I - V characteristic when both Pb and Al are superconducting. Curve A represents data obtained with a power supply of large internal impedance. Curve B presents an expanded view of the negative differential conductance region when a low-impedance supply was employed. The two half-energy-gap values indicated are very close to those obtained by Townsend and Sutton.

³² A. S. Joseph and W. J. Tomasch, Phys. Rev. Letters 12, 219 (1964).

inset of Fig. 7, zero diode conductance for $V > \epsilon_2(H=0)$ was generally observed for fields considerably in excess of H_{c1} . Within the precision permitted by the broadness of feature E (Fig. 1), ϵ_M approximately equals $\epsilon_1(H=0)$. For the thin Al films used, ϵ_2 (Fig. 7) is seen to remain essentially constant over the field range in which structure was resolvable.

Within experimental accuracy, the zero-field alloy energy gap (1.1°K) is independent of composition, maintaining a value of $2.66 \pm 0.04 \times 10^{-3}$ eV which is very near that reported for pure Pb.³ [Estimates based on the BCS^{32a} functional form of $\epsilon(T)$ indicate that the energy gap values obtained at 1.1°K are essentially equal to $\epsilon(0)$ within the indicated experimental uncertainty.] This numerical result summarizes measurements made on seven alloys (Table I), and is in satisfactory agreement with values obtained from infrared absorption measurements³³ made below 10 at.% Tl ($2.66 \pm 0.04 \times 10^{-3}$ eV at 7.7 at.% Tl). On the other hand, the substantial decrease in the infrared energy gap³³ to $2.44 \pm 0.04 \times 10^{-3}$ eV at 10.0 at.% Tl was not observed in tunneling measurements made at 9.4 and 9.6 at.% Tl, nor was an atypical energy gap observed at 13.5 at.% Tl. The source of this difference is not understood.

Attempts to observe ϵ_m for thick pure Pb films have been frustrated by complications stemming from the existence of two well-resolved energy gaps, the situation being depicted in Fig. 8. This effect has been discussed previously by Townsend and Sutton^{10,13} who suggest that the two energy gaps are associated with different portions of the Fermi surface, corresponding to electronic occupancy of different order Brillouin zones. The absence of such complications for the present alloys is

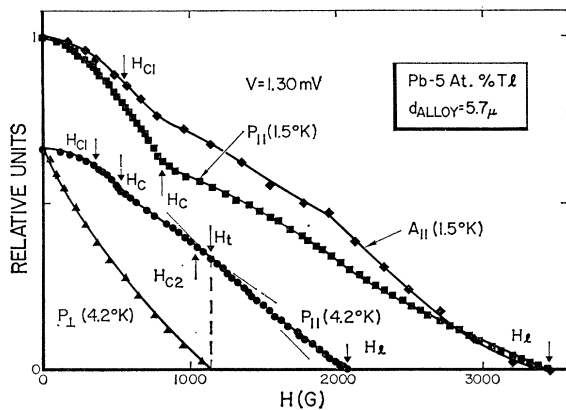


FIG. 9. Field dependence of A_{II} , P_{II} , and P_I at two temperatures. Plots of $A_{II}(4.2^\circ\text{K})$ and $P_I(1.5^\circ\text{K})$ have been omitted for clarity. Indicated bulk critical field values at 1.5°K were calculated from measured values at 4.2°K which are also indicated.

^{32a} J. Bardeen, L. N. Cooper, and J. R. Schrieffer, Phys. Rev. **108**, 1175 (1957).

³³ J. D. Leslie and D. M. Ginsberg, Phys. Rev. **133**, A362 (1964).

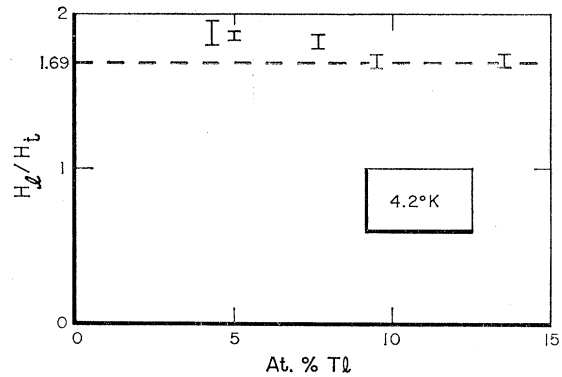


FIG. 10. The ratio H_I/H_t versus alloy composition. The theoretical value of H_{c3}/H_{c2} predicted by Saint-James and de Gennes is indicated by a dashed line. Results obtained for the same films at 1.5°K have not been plotted since they are identical to those obtained at 4.2°K within experimental accuracy.

consistent with expectations based on the theory of dirty superconductors.³⁴

B. Aluminum Normal

Figure 9 presents A_{II} , P_{II} , and P_I data for a particular diode at two different temperatures. Again, these results are representative (5.0, 7.9, and 13.5 at.% Tl), and previous comments regarding reproducibility hold here also. Bulk critical field values (H_{c1} and H_c) at 1.5°K were obtained from 4.2°K magnetization values by parabolic extrapolation as mentioned earlier. Longitudinal field results appear to be independent of the relative orientation of H_{II} and the direction of the film conduction current. All the features of Fig. 5 are easily recognized in Fig. 9, with the addition that P_{II} slightly exceeds A_{II} near H_t for this particular diode. Comparison of Figs. 6 and 9 emphasizes the differences between type-I and type-II behavior (in a field) as evidenced by tunneling.

All diodes investigated displayed constant field $I-V$ curves which crossed the Ohmic limit near $V = 4.8 \times 10^{-3}$ eV, remaining slightly above the limit until merger at approximately 15×10^{-3} eV. This behavior is almost certainly attributable to anomalies in $N(E)$ produced by peaks in the lattice vibration spectrum.^{7,15} For simplicity, the area of the closed figure formed by a constant field $I-V$ curve and the Ohmic limit ($0 \leq V \leq 5 \times 10^{-3}$ V) was taken as an approximation of $A_{II}(H)$. This procedure should introduce generally negligible errors, perhaps resulting in a small underestimate of $A_{II}(H)$ at the highest fields.

Figure 10 presents the ratio H_I/H_t at 4.2°K, as determined from P_{II} and P_I for five alloys as a function of composition. It is seen to depend but weakly on Tl concentration, with perhaps some evidence for a tendency to increase with decreasing Tl content. To within

³⁴ P. W. Anderson, J. Phys. Chem. Solids **11**, 26 (1959).

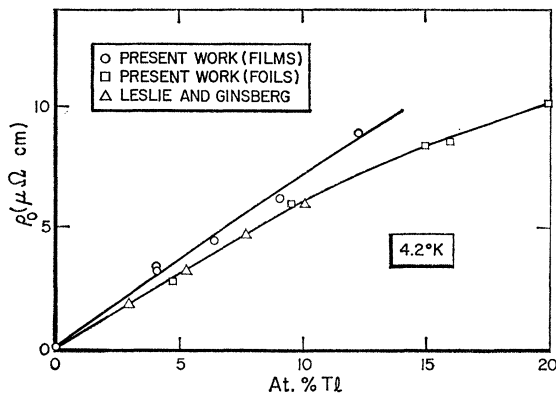


FIG. 11. Electrical resistivity of Pb-Tl alloys in foil and film form. Data of Leslie and Ginsburg (see footnote 33) correspond to resistivity of well-annealed massive samples.

experimental accuracy, this ratio was independent of temperature down to 1.5°K.

C. Alloy Normal

A knowledge of alloy film resistivities (4.2°K), relative to bulk values, will prove valuable. Such measurements were performed on unannealed films and on well-annealed foils, results being summarized in Fig. 11. Measurements made on well-annealed massive specimens³³ are included for comparison, and there is good agreement between these and the foil results. Film resistivities, however, tend to systematically exceed bulk values by approximately 15–20%. This is most likely attributable to the method of film formation, since even very pure evaporated thick films commonly behave in this way, although annealing often improves the situation substantially. In view of the present residual pressures and deposition rates during fabrication, the increased resistivity is believed to be due to lattice imperfections rather than chemical contamination. Unfortunately, diodes can be ruined by even rather modest attempts at annealing.

V. DISCUSSION AND SUMMARY

A. Aluminum Superconducting and No Applied Field

The observed existence of a sharply defined alloy energy gap is consistent with the Anderson theory of dirty superconductors.³⁴ Present measurements indicate that the energy gap is essentially independent of composition in the range 0–13.5 at. % Tl. Below 10.0 at. % Tl, satisfactory agreement exists between tunneling and infrared data.³³ The substantial depression (8.5%) of the infrared energy gap value at 10.0 at. % Tl is not reflected in the tunneling data, and the origin of this difference remains unexplained.

Existing bulk magnetization data^{27–29} indicate that H_c , and hence the condensation energy, also remains

essentially constant ($\pm 2\%$) to at least 10 at. % Tl. This is in harmony with the present observed constancy of the energy gap provided the density of states at the Fermi level $N(0)$ is nearly unaffected by alloying. The linear relationship between H_{c2} and the residual resistivity ρ_0 observed by Livingston²⁸ for 4.78–30.1 at. % Tl, when interpreted in terms of the approximate Gor'kov-Goodman equation^{35,36} ($H_{c2}H_c^{-1} \doteq \text{constant } \gamma^{1/2}\rho_0$), implies that $N(0)$ is indeed insensitive to alloying.

B. Aluminum Superconducting in a Field

Cooling a tunnel diode in zero field from a temperature at which both films are normal, to one at which both are superconducting, produces a dramatic increase in the diode junction impedance for $V < (\epsilon_1 + \epsilon_2)$. This now familiar phenomenon^{1,2} is entirely attributable to the existence of energy gaps in *both* superconductors. The inset of Fig. 7 indicates that the junction impedance can remain very large relative to the Ohmic limit even when $H \approx 2H_c$, implying that all of the alloy involved in zero-field tunneling retains a sizeable energy gap to at least such fields. Furthermore, since the impedance remains very large for $V < V_B$ (Fig. 2) and decreases quite rapidly beyond V_D , it would appear that the minimum alloy energy gap satisfies $V_B < \epsilon_m < V_D$. These inferences appear quite general, depending only on the notion of an energy gap in $N(E)$.

Structural features in the present data (Figs. 1 and 2) may be accounted for in a simple way by means of a model which postulates a spectrum of field-induced energy gaps $2\epsilon_i$ such that $\epsilon_m \leq \epsilon_i \leq \epsilon_M$. By virtue of their thinness, the Al films can be characterized by a single energy gap.^{9,18,19} Any small volume element within the surface layer is then characterized by a definite value of ϵ_i , and is naively assumed to produce an I - V plot similar to that of Fig. 1 ($H=0$) with ϵ_1 replaced by ϵ_i . To obtain the net I - V diode characteristic, a weighted sum must be taken over all contributing volume elements, where the weighting factor reflects the relative tunneling probability and presumably decreases with increasing distance from the surface. Details of the weighting process are not important here so long as the process is sufficiently smooth so as not to introduce additional structure by itself. For present purposes, this sum need be formed only in principle.

Structural features which appear in Figs. 1 and 2 may now be tentatively interpreted as follows: Region *A* constitutes a smooth background corresponding to V being reasonably smaller than ϵ_m , which is in turn reasonably larger than ϵ_2 . The sharp rise in I associated with ϵ_m just prior to $V = \epsilon_m - \epsilon_2$ (Fig. 2, $H=0$) produces feature *B*. Point *C* is identified with $V_C = \epsilon_m - \epsilon_2$, with I rising less rapidly thereafter since volume elements of small ϵ_i have entered the negative differential conduct-

³⁵ L. P. Gor'kov, Zh. Eksperim. i Teor. Fiz. **37**, 1407 (1959) [English transl.: Soviet Phys.—JETP **10**, 998 (1960)].

³⁶ B. B. Goodman, IBM J. Res. Develop. **6**, 63 (1962).

ance portion of their I - V characteristic. Point D is identified with $V_D = \epsilon_m + \epsilon_2$, with I rising more rapidly thereafter. Finally, I rises less rapidly above $V_B = \epsilon_M + \epsilon_2$ as all contributions from the active layer smoothly tend to the Ohmic limit. So long as the structural features of Figs. 1 and 2 are observable, the foregoing rationale permits experimental evaluation of ϵ_m , ϵ_M , and ϵ_2 , as in Fig. 7. In view of recent studies on thin Al films,¹⁹ identification of $\epsilon_2(H)$ with the Al energy gap seems quite reasonable. Furthermore, the observed behavior of ϵ_m and ϵ_M seems to be in harmony with a simple physical picture based on the Ginzburg-Landau-Abrikosov-Gor'kov³⁷⁻⁴⁰ theory of type-II superconductivity as, will be indicated.

For purposes of discussion, the thick alloy film is replaced by a superconducting half-space with a magnetic field applied parallel to the planar vacuum-superconductor interface. Taking any point on the interface as an origin of orthogonal coordinates (x, y, z) , the x axis lies in the interface parallel to H , while the z axis is normal to the interface, being positive within the superconductor. The Ginzburg-Landau (G-L) order parameter³⁷ Ψ is assumed to be proportional to the energy gap,⁴⁰ both being normalized with respect to their zero-field values. For the present concentrations and temperatures, the electronic coherence length ξ and the mean free path L are approximately equal. Tunneling electrons are assumed to originate within a layer $0 \leq z \leq L \approx \xi$. For the Meissner state ($0 < H_{||} < H_{c1}$), the parameter Ψ presumably depends only on z , rising from a minimum value ϵ_s at the surface,⁴¹ to approximately unity near $z = L \approx \xi$. Consequently, tunneling electrons are expected to exhibit a spectrum of energy gaps bounded by ϵ_s and $\epsilon_1(H=0)$, which is consistent with experimental observations provided ϵ_s is identified with ϵ_m .

Ideally, flux penetration in the form of vortex tubes having axes parallel to x should occur at H_{c1} , the mixed phase lower stability limit. For the present, it will be assumed that the vortex lattice³⁹ has been established for fields slightly greater than H_{c1} . The boundary condition that no paired electrons cross the interface requires that a current sheet separate the vortex lattice from the interface. In view of this, it may be that Ψ is only weakly modulated near the interface. If this is the case, flux penetration above H_{c1} need not result in the rapid dissolution of the structure observed at lower fields (V_C , V_D , and V_B of Figs. 1 and 2). Such structure might be intrinsically present throughout the mixed

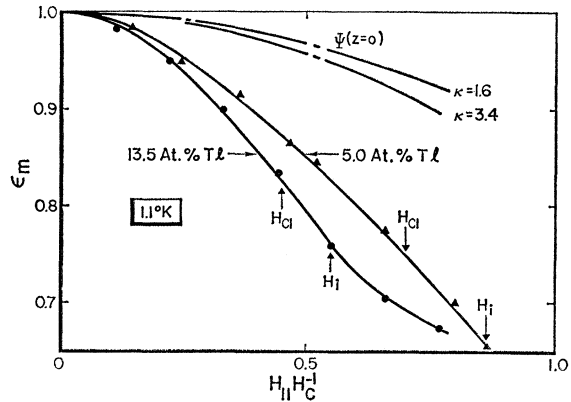


Fig. 12. Expanded plot of $\epsilon_m(H)$ for the extreme alloy compositions studied. Field values corresponding to inflection points are denoted by H_i . Broken lines indicate calculated values of the low-field G-L order parameter $\Psi(z=0)$ (see footnotes 37 and 41). Appropriate κ values were obtained from Fig. 15.

state, although the present data give no indication that this is actually the case. On the other hand, considerable refinement in experimental technique would be required before it would be safe to conclude that such structure is intrinsically absent at higher fields than those presently reported. Future measurements may clarify this point.

Although the Ginzburg-Landau-Abrikosov picture envisages a sharp termination of the Meissner state at H_{c1} , torque magnetometer studies³² indicate that for alloy films similar to those currently employed, flux entry is postponed to fields substantially higher than H_{c1} . (Simple estimates indicate that even the thinnest film studied was still sufficiently thick to accommodate several vortex layers at H_{c1} .) Subsequent scoring of these films with a sharply pointed tool results in flux entry at the bulk value of H_{c1} .³² These results are predicted by the theory of Bean and Livingston⁴² which attributes flux delay phenomena to the effect of vortex image forces which presumably become important in the vicinity of a surface. Pronounced effects are presumably absent in most bulk experiments due to surface roughness, scratches and the like, which serve as flux injection centers. Qualitatively, this picture seems quite reasonable, although estimates of the fields to which such delay may persist seem significantly smaller than those observed. It would appear that delayed entry of flux phenomena are important in the present experimental situation.

To the extent that delayed flux entry may be viewed as the metastable retention of the Meissner state, the field dependence of ϵ_m just beyond H_{c1} might well be expected to be a continuation of the variation observed below H_{c1} , much as in Figs. 7 and 12. As $(H_{||} - H_{c1})H_{c1}^{-1}$ becomes increasingly large, however, ϵ_m is observed to suffer a change in character as evidenced by the occur-

³⁷ V. L. Ginzburg and L. D. Landau, *Zh. Eksperim. i Teor. Fiz.* **20**, 1064 (1950).

³⁸ V. L. Ginzburg, *Nuovo Cimento* **2**, 1234 (1955).

³⁹ A. A. Abrikosov, *Zh. Eksperim. i Teor. Fiz.* **32**, 1442 (1957) [English transl.: *Soviet Phys.—JETP* **5**, 1174 (1957)].

⁴⁰ L. P. Gor'kov, *Zh. Eksperim. i Teor. Fiz.* **37**, 1407 (1959) [English transl.: *Soviet Phys.—JETP* **10**, 998 (1960)].

⁴¹ Consult E. A. Lynton, *Superconductivity* (John Wiley & Sons, Inc., New York, 1962), p. 51. Analytical solutions of the one-dimension G-L equations for $(\kappa H^2/H_c^2) \ll 1$ have this general character.

⁴² C. P. Bean and J. D. Livingston, *Phys. Rev. Letters* **12**, 14 (1964).

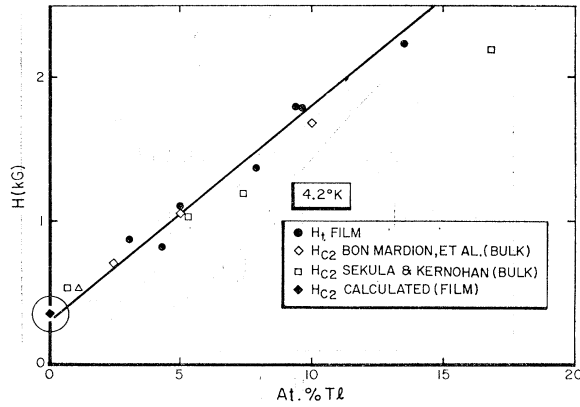


FIG. 13. Dependence of $H_t(4.2^\circ\text{K})$ on alloy composition. Bulk values of $H_{c2}(4.2^\circ\text{K})$ have been included for comparison (see footnotes 27-29). The film result for $\rho_0=0$ was calculated from $H_t(\text{Pb})$ employing theory of Saint-James and de Gennes.

rence of an inflection point (Fig. 12) for fields in the range $1.2 \leq H_{11}/H_{c1} \leq 1.4$. (This numerical result is based on data obtained with three diodes having compositions 5.0, 7.9, and 13.5 at.% Tl.) Since H_{11}/H_{c1} is an index of the degree of metastability present, the foregoing may be taken as an indication that ϵ_m changes character when a certain critical degree of metastability is achieved. Two opposed interpretations are possible depending on whether the change in $\epsilon_m(H)$ is attributed to (1) the onset of flux entry, or (2) an increasing departure from equilibrium produced by the continued postponement of flux entry. Two possible and divergent interpretations serve to illustrate: (1) sharp I - V structure (V_C , V_D , and V_E of Figs. 1 and 2) persists beyond vortex penetration, although the field dependence of ϵ_m is altered from that of the Meissner state, or (2) structure is retained only so long as the Meissner state is retained, disappearing upon the onset of flux entry. Although a small amount of circumstantial evidence favoring the latter trend is available, the present data do not strongly suggest a preference for one trend over the other. The significance of the eventual loss of structure remains an open issue at this time. Many of these points may yield to continued study.

As indicated earlier, qualitative interpretation of the present data seems straightforward within the confines of the equilibrium Meissner state ($H_{11} < H_{c1}$). Figure 12 presents an expanded plot of ϵ_m versus H/H_c , for the most dilute and the most concentrated alloy. It is interesting to compare these data with the quantitative predictions of the G-L theory, even though the condition $(1 - TT_c^{-1}) \ll 1$ is not satisfied. Analytical solutions for the one-dimensional problem are available³⁷ subject to the conditions $HH_c^{-1} \ll \sqrt{2}$ and $\kappa(H/H_c)^2 \ll 1$, corresponding to $\Psi(z=0)$ being only slightly perturbed from unity. It is noteworthy that $\kappa \ll 1$ need not be satisfied so long as the previous inequalities hold. For the alloys in question, these conditions are met for fields satisfying $0 \leq HH_c^{-1} < 0.2$. Observed ϵ_m values (Fig. 12) are seen

to drop more rapidly than $\Psi(z=0)$ evaluated for appropriate κ values. Such behavior may be attributable to the inapplicability of the G-L equation at these low temperatures, although other contributing factors cannot be ruled out,⁴³ including the possibility that the boundary conditions at a superconductor-oxide interface differ significantly from the superconductor-vacuum ideal.

C. Aluminum Normal for All Fields

A comparison of film H_t data (obtained from P_{11}) and bulk H_{c2} data, both plotted as a function of composition, is presented in Fig. 13. Below approximately 10 at.% Tl, H_t and H_{c2} are equal to within experimental accuracy. With the aid of the curves of Fig. 11, these same field data are replotted as a function of ρ_0 (residual resistivity) in Fig. 14. On this basis, good agreement is achieved for all compositions studied. Justification for this mode of intercomparison can be found in the data of Livingston²⁸ which indicate a linear relationship between H_{c2}/H_c and ρ_0 (in accord with predictions based on the Gor'kov-Goodman equation) for a variety of Pb based alloys, including several different solutes, and spanning a large concentration interval. The agreement between H_t and H_{c2} (bulk) (Fig. 14) is taken as evidence that the present results are generally typical of bulk specimens.

Contrary to the predictions of the G-L theory for an unbounded type-II superconductor, the cessation of superconductivity (as evidenced by tunneling in this instance) does not occur at $H_{11} = H_{c2}$, since both A_{11} and P_{11} retain a sizeable fraction (35-45%) of their zero-

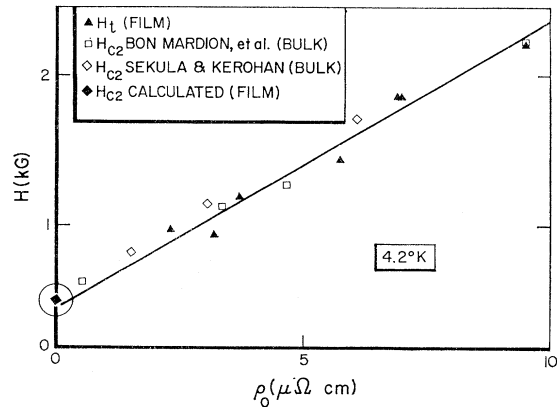


FIG. 14. Dependence of $H_t(4.2^\circ\text{K})$ on residual resistivity ρ_0 . Bulk values of $H_{c2}(4.2^\circ\text{K})$ have been included for comparison (see footnotes 27-29). Data of Fig. 11 were employed to effect conversion from composition to ρ_0 . The film result for $\rho_0=0$ was calculated from $H_t(\text{Pb})$ employing theory of Saint-James and de Gennes.

⁴³ In principle, qualitatively similar effects could result from a systematic misalignment between specimen and field. Sharpness of the S-N transition for pure Pb (Fig. 6), and the very large diode impedance ($V=0$) for high fields (inset of Fig. 7), indicating the absence of normal material, are offered as evidence that this source of error is unlikely.

field value at H_{c2} (Fig. 9). Such behavior suggests that much of the alloy active in zero-field tunneling retains a sizeable energy gap at H_{c2} , the last vestige of superconductivity being lost at H_t . Since H_t has been identified with H_{c2} , the data of Fig. 10 imply that H_t is also intimately linked to H_{c2} , the ratio H_t/H_{c2} being independent of temperature (1.4–4.2°K) and thickness (2.5–7.5 μ), and nearly independent of composition ($1.7 \leq H_t H_{c2}^{-1} \leq 1.9$). In view of this, it is believed that H_t reflects the presence of a basic effect rather than one caused by specimen defects of various kinds. Hence, the present data indicate the persistence of superconductivity within a coherence length of the surface over an interval $H_{c2} \leq H_{t1} \leq H_t$. Again, the relatively large values of $A_{11}(H_{c2})$ and $P_{11}(H_{c2})$ imply that a large fraction of the diode area participates. Finally, the smooth variation of A_{11} and P_{11} in the vicinity of H_{c2} suggests that no drastic changes near the surface attend the quenching of superconductivity within the bulk of the alloy film.

Saint-James and de Gennes⁴⁴ have examined the influence of a planar boundary on the solutions of the G-L equations at high fields, and have concluded that a superconducting lamellar region or *sheath* exists at the surface for longitudinal fields satisfying $H_{c2} \leq H_{t1} \leq H_{c3} = 1.69H_{c2}$, the sheath being roughly a coherence length

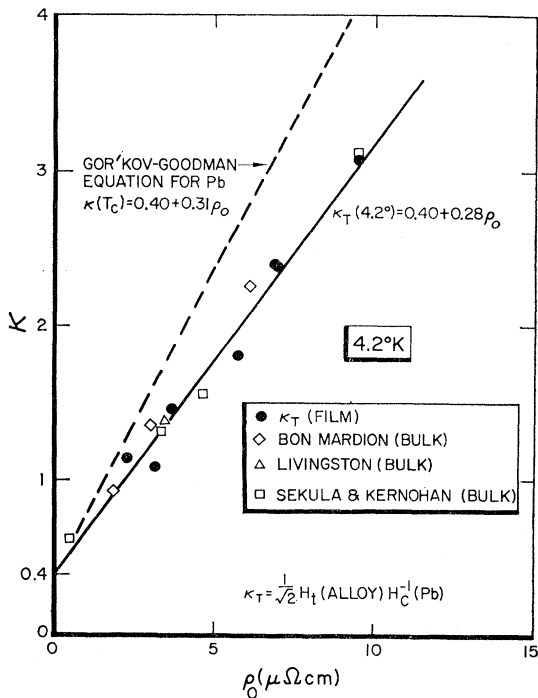


FIG. 15. Dependence of G-L parameter κ on residual resistivity ρ_0 . Bulk values of κ (see footnotes 27–29) have been included for comparison with κ_T obtained from film-tunneling data. Data of Fig. 11 were employed to effect the conversion from composition to ρ_0 .

⁴⁴ D. Saint-James and P. G. deGennes, Phys. Letters 7, 306 (1963).

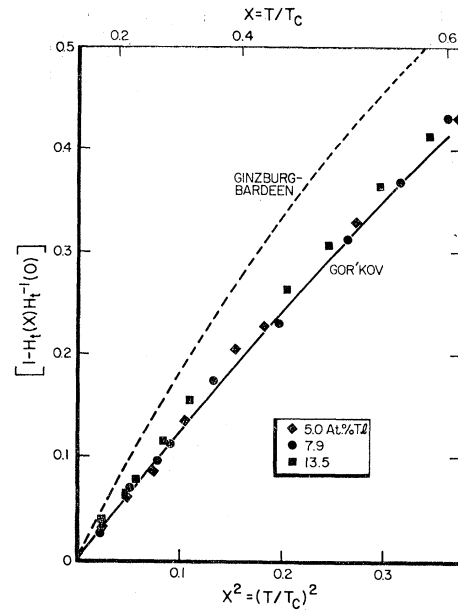


FIG. 16. Temperature dependence of H_t for three alloy films. Two theoretical predictions for the temperature dependence of H_{c2} are also indicated. Reduced temperatures were calculated utilizing the alloy critical temperature data of Finnemore and Mapother as quoted in the reference of footnote 33.

in depth. For transverse fields, they conclude that the sheath phase is not formed, all superconductivity terminating at H_{c2} instead.

This theoretical picture appears to provide a reasonably good quantitative account of the present observations. The specific points of agreement are as follows: (1) $H_t H_t^{-1} \approx 1.7$, (2) $H_t \approx H_{c2}$, and (3) $H_t H_t^{-1}$ is not a function of temperature. For the two highest compositions studied, H_t/H_t equaled 1.7 within experimental accuracy (Fig. 10). Values for the remaining alloys, however, exceed this value by as much as eleven percent. Torque measurements on well-annealed but otherwise similar films^{45,46} have yielded better agreement with theory down to 4.2 at. % Tl. Limitations imposed by practical considerations, such as small angular misalignments of field, are not easily invoked to account for the present tunneling results since such factors tend generally to decrease, not increase, the ratio H_t/H_t . In view of the fact that H_t/H_t is at best a weak function of ρ_0 , it is difficult to see how annealing effects could account for the observed differences. Generally speaking, however, the quantitative agreement with Saint-James and de Gennes is considered to be satisfactory.

A more detailed look at the data for pure Pb (Fig. 6) is warranted at this point. As a practical matter, Pb films tend to anneal at room temperature, aged films exhibiting resistance ratios (300°K/4.2°K) of 500 or more. Despite this convenience, the tail above H_c is

⁴⁵ W. J. Tomasch and A. S. Joseph, Phys. Rev. Letters 6, 148 (1964).

⁴⁶ A. S. Joseph and W. J. Tomasch (to be published).

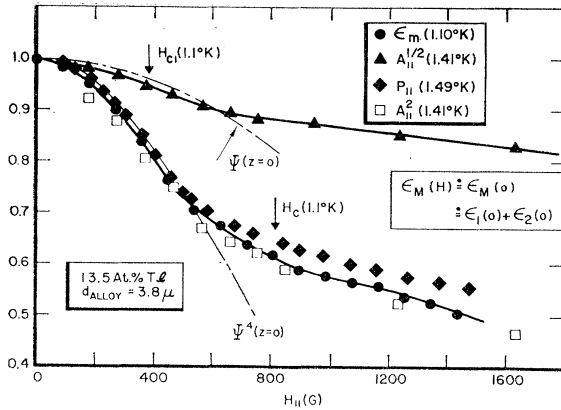


FIG. 17. Field dependence of ϵ_m , P_{11} , $A_{11}^{1/2}$, and A_{11}^2 . Note suppression of ordinate zero. The calculated low-field G-L order parameter $\Psi(z=0)$ (see footnotes 37 and 41) and $\Psi^4(z=0)$ have also been included. Indicated critical fields were calculated from 4.2°K bulk data.

consistently observed for thick films, independent of thickness and particulars of manufacture. The general regularity and reproducibility of these data suggest the presence of a genuine effect. According to Saint-James and de Gennes the inequality $H_{c3} \geq H_c \geq H_{c2}$ can be satisfied provided κ lies in the range $0.419 \leq \kappa \leq 0.707$. To see whether H_l could be identified with H_{c3} , the quantity H_{c2} was calculated from $H_l H_{c2}^{-1} = 1.7$. Figure 14 contrasts this calculated value with $H_l(\rho=0)$ obtained by extrapolating the alloy data. The agreement is good although it can be improved by taking H_{c3}/H_{c2} as 1.9 rather than 1.7, which could be interpreted as further evidence of a concentration effect as suggested in Fig. 10. Hence for Pb, the sheath phase appears to be stable ($H_c \leq H_{11} \leq H_l$), while the mixed phase is not. Torque magnetometer studies⁴⁶ on foils have yielded similar results, as have a number of other measurements.^{21,30,31} The abrupt transition from the Meissner state to the sheath state at H_c (bulk) probably reflects the ineffectiveness of the sheath in inhibiting rapid flux entry. It is noted in passing that $\Psi(z=0)$ provides a reasonable fit to the $A^{1/2}$ data of Fig. 6.

As mentioned previously, $N(0)$ appears to be rather insensitive to alloying. Consequently, the essential constancy of the energy gap, as observed by tunneling in zero field, may be interpreted as indicating that H_c remains essentially constant at the value for pure Pb, a conclusion supported by bulk magnetization data.²⁷⁻²⁹ Hence what could be called an all-tunneling κ value can be calculated from the relationship $\kappa_T = H_l(\text{alloy}) \times [\sqrt{2}H_c(\text{Pb})]^{-1}$. Figure 15 depicts the ρ_0 dependence of κ_T , and agreement with bulk magnetization values is seen to be good. Several predictions exist for the temperature dependence of H_{c2} , two of which⁴⁷⁻⁴⁹ are in-

⁴⁷ J. Bardeen, Phys. Rev. **95**, 554 (1954).

⁴⁸ V. L. Ginzburg, Zh. Eksperim. i Teor. Fiz. **30**, 593 (1956) [English transl.: Soviet Phys.—JETP **3**, 621 (1956)]; Dokl.

cluded in Fig. 16 for comparison with the H_l data. Rather good agreement exists between these data and the Gor'kov prediction.⁵⁰

D. Comparison of Results Obtained Above and Below T_c (Al)

Plots of ϵ_m , P_{11} , and $A_{11}^{1/2}$ and A_{11}^2 versus H for a particular diode appear in Fig. 17, these results being representative of those obtained for all compositions studied in detail (5.0, 7.9, and 13.5 at.% Tl). It should be noted that the ϵ_m data were obtained at a slightly lower temperature than the rest. A striking feature of these plots is the close numerical agreement between ϵ_m , P_{11} , A_{11}^2 , and $\Psi^4(z=0)$. No explanation is offered for these empirical regularities. Most intriguing is the correlation between P_{11} and ϵ_m , the possibility being that P_{11} is proportional to the surface energy gap over a considerable range of field. Whether or not this correlation persists to significantly higher fields than indicated is of course an open issue in view of the present inability to chart ϵ_m further.

E. Interpretation of A_{11} at Low Fields

Several elemental superconductors, including Pb, have been found to exhibit zero-field differential conductances (dI/dV versus V) which are quite nearly proportional to the BCS density of states,^{1,3,7,12,13} and theoretical justifications for this result have been put forward by several authors.⁵¹⁻⁵³ Although careful comparisons between alloy dI/dV curves (taken at low temperatures and zero field) and the BCS function have not been made, graphical differentiation of present $I-V$ plots yields curves of quite similar character.^{53a} In view of the foregoing, it appears reasonable to postulate that dI/dV is proportional to the quasiparticle density of states under the conditions to be discussed. Assuming this view, arguments can be made which indicate that A_{11} is approximately proportional to the energy gap $\epsilon(0)$ at low temperatures and zero field, or to an average energy gap⁵⁴ $\langle \epsilon \rangle$ when a small longitudinal field is applied, the averaging being the result of the spatial variation of the energy gap over a coherence length.

To begin with, it is convenient to define a quantity

Akad. Nauk SSSR **110**, 368 (1956) [English transl.: Soviet Phys.—Doklady **1**, 541 (1956)].

⁴⁹ L. P. Gor'kov, Zh. Eksperim. i Teor. Fiz. **37**, 833 (1959) [English transl.: Soviet Phys.—JETP **10**, 593 (1960)].

⁵⁰ For a discussion of the temperature dependence of κ for dilute Pb-Tl alloys, consult M. Cardona and B. Rosenblum, Proceedings of the Ninth International Conference on Low Temperature Physics, Columbus, Ohio, 1964 (to be published); also, B. Rosenblum and M. Cardona, Phys. Letters (to be published).

⁵¹ J. Bardeen, Phys. Rev. Letters **6**, 57 (1961).

⁵² M. H. Cohen, L. M. Falicov, and J. C. Phillips, Phys. Rev. Letters **8**, 316 (1962).

⁵³ J. Bardeen, Phys. Rev. Letters **9**, 147 (1962).

^{53a} Recently acquired data indicate good agreement between dI/dV and the BCS function for $0 \leq V < 2\epsilon_1$. At higher voltages, phonon effects are observed as in Pb.

⁵⁴ L. Dubeck, P. Lindemfeld, E. A. Lynton, and H. Rohrer, Phys. Rev. Letters **10**, 98 (1963).

γ as follows:

$$\gamma = \int_0^{\hbar\omega_c} N(E)E dE = e^2 \int_0^{V_c} N(V)V dV, \quad (1)$$

where N is the density of states function, and ω_c is a cutoff frequency associated with the electron-phonon interaction, being related to the Debye temperature by the relationship $\hbar\omega_c \approx k\Theta_D$. Invoking the proportionality between dI/dV and N , and taking the difference between γ in the superconducting and normal states yields

$$\begin{aligned} \gamma_{SN} &= \frac{e^2}{g} \int_0^{I_c} (V_S - V_N) dI = \frac{e^2}{g} A_{11}(0) \\ &= \int_0^{\hbar\omega_c} (N_S - N_N) E dE, \end{aligned} \quad (2)$$

where g is a constant of proportionality, $A_{11}(0)$ is the area between the zero-field I - V curve and the Ohmic limit, and I_c is related to V_c via the observed I - V diode characteristic. It should be noted that this relationship between $A_{11}(0)$ and $(N_S - N_N)$ depends only on the assumed proportionality of dI/dV and N , and the particular choice of ω_c . The general form of the integral indicates that $A_{11}(0)$ does indeed reflect the degree of superconductivity present. To proceed further, however, requires a knowledge of $N_S(E, H)$, the simplest choice being the BCS function for $T=0$ and $H=0$.

$$\begin{aligned} \gamma_{SN} &= N(0) \int_{\epsilon(0)}^{\hbar\omega_c} [E^2 - \epsilon^2(0)]^{-1/2} E^2 dE \\ &\quad - N(0) \int_0^{\hbar\omega_c} E dE. \end{aligned} \quad (3)$$

Integrating, and making use of the fact that $[2\hbar\omega_c/\epsilon(0)] \gg 1$ allows $A_{11}(0)$ to be written as

$$A_{11}(0) = (g/e^2) [\frac{1}{2} N(0) \epsilon^2(0)] \ln [2\hbar\omega_c/\epsilon(0)]. \quad (4)$$

Since the logarithmic factor is a relatively slow function of $\epsilon(0)$, this form indicates that $A_{11}(0)$ is approximately proportional to the BCS condensation energy

$\frac{1}{2} N(0) \epsilon(0)^2$. The influence of an applied field is felt through the changes induced in $N(E)$, which has its sharp features progressively degraded. Differential conductance measurements on pure Pb by Goldstein²¹ indicate that these effects are fairly small below about $\frac{1}{2} H_c$. Since the order parameter is somewhat less rigid in the alloys, the effect will tend to be greater than in pure Pb. In part, this situation may be improved by replacing ϵ by an average energy gap parameter $\langle \epsilon \rangle$, so that Eq. (4) can be recast as

$$A_{11}(H) = \langle \epsilon(H) \rangle^2 \left\{ 1 + [1 - \langle \epsilon(H) \rangle] / \ln \left(\frac{2\hbar\omega_c}{\epsilon(0)} \right) \right\}, \quad (5)$$

where A_{11} and $\langle \epsilon \rangle$ have been renormalized with respect to zero-field values, and $(1 - \langle \epsilon \rangle)$ has been taken to be substantially less than unity. Introducing numerical constants appropriate to Pb yields

$$A_{11}^{1/2}(H) = \langle \epsilon(H) \rangle \{ 1 - 0.3 [1 - \langle \epsilon(H) \rangle] \}. \quad (6)$$

It is difficult to determine the range of field over which Eq. (6) should be applicable. Judging from the behavior of $N(E)$ pure Pb,²¹ an estimate of $HH_c^{-1} < 0.2$ may be reasonable. As indicated in Fig. 17, $A_{11}^{1/2}$ lies intermediate between ϵ_m and unity. This is as it should be if $A_{11}^{1/2}$ is to be associated with an average energy gap. The relatively rapid separation of ϵ_m and $A_{11}^{1/2}$ is presumably due to the increased flexibility of the order parameter produced by alloying, causing the average to substantially exceed the minimum. It could be argued that the pure Pb data of Fig. 6 support this view (assuming P_{11} to be proportional to ϵ_m as it is in the alloys) since $A_{11}^{1/2}$ and P_{11} diverge by a comparatively small amount even at H_c . It is interesting to note that the G-L expression for $\Psi(z=0)$ provides a reasonable fit to the low field $A_{11}^{1/2}$ data over the composition range studied (Figs. 6 and 17).

ACKNOWLEDGMENTS

The author wishes to thank T. G. Berlincourt, A. S. Joseph, and R. R. Hake for many helpful discussions, as well as R. R. Hargrove for aid with specimen preparation and E. P. Parry for the chemical analyses.